# Conserved Tyrosine-369 in the Active Site of *Escherichia coli* Copper Amine Oxidase Is Not Essential[†,‡]

Jeremy M. Murray,[§] Christian R. Kurtis, Winston Tambyrajah,[||] Colin G. Saysell, Carrie M. Wilmot,[⊥] Mark R. Parsons, Simon E. V. Phillips, Peter F. Knowles, and Michael J. McPherson*

*Astbury Centre for Structural Molecular Biology, School of Biochemistry and Molecular Biology, University of Leeds, Leeds LS2 9JT, United Kingdom*

*Received June 8, 2001; Revised Manuscript Received August 21, 2001*

ABSTRACT: Copper amine oxidases are homodimeric enzymes that catalyze two reactions: first, a self-processing reaction to generate the 2,4,5-trihydroxyphenylalanine (TPQ) cofactor from an active site tyrosine by a single turnover mechanism; second, the oxidative deamination of primary amine substrates with the production of aldehyde, hydrogen peroxide, and ammonia catalyzed by the mature enzyme. The importance of active site residues in both of these processes has been investigated by structural studies and site-directed mutagenesis in enzymes from various organisms. One conserved residue is a tyrosine, Tyr369 in the *Escherichia coli* enzyme, whose hydroxyl is hydrogen bonded to the O4 of TPQ. To explore the importance of this site, we have studied a mutant enzyme in which Tyr369 has been mutated to a phenylalanine. We have determined the X-ray crystal structure of this variant enzyme to 2.1 Å resolution, which reveals that TPQ adopts a predominant nonproductive conformation in the resting enzyme. Reaction of the enzyme with the irreversible inhibitor 2-hydrazinopyridine (2-HP) reveals differences in the reactivity of Y369F compared with wild type with more efficient formation of an adduct ($\lambda_{max}$ = 525 nm) perhaps reflecting increased mobility of the TPQ adduct within the active site of Y369F. Titration with 2-HP also reveals that both wild type and Y369F contain one TPQ per monomer, indicating that Tyr369 is not essential for TPQ formation, although we have not measured the rate of TPQ biogenesis. The UV−vis spectrum of the Y369F protein shows a broader peak and red-shifted $\lambda_{max}$ at 496 nm compared with wild type (480 nm), consistent with an altered electronic structure of TPQ. Steady-state kinetic measurements reveal that Y369F has decreased catalytic activity particularly below pH 6.5 while the $K_M$ for substrate $\beta$-phenethylamine increases significantly, apparently due to an elevated p$K_a$ (5.75−6.5) for the catalytic base, Asp383, that should be deprotonated for efficient binding of protonated substrate. At pH 7.0, the $K_M$ for wild type and Y369F are similar at 1.2 and 1.5 $\mu$M, respectively, while $k_{cat}$ is decreased from 15 $s^{-1}$ in wild type to 0.38 $s^{-1}$, resulting in a 50-fold decrease in $k_{cat}/K_M$ for Y369F. Transient kinetics experiments indicate that while the initial stages of enzyme reduction are slower in the variant, these do not represent the rate-limiting step. Previous structural and solution studies have implicated Tyr369 as a component of a proton shuttle from TPQ to dioxygen. The moderate changes in kinetic parameters observed for the Y369F variant indicate that if this is the case, then the absence of the Tyr369 hydroxyl can be compensated for efficiently within the active site.

Copper amine oxidases (CuAOs;[1] E.C. 1.4.3.6) have diverse biological functions including nutrient metabolism in prokaryotes (*1*−*3*) and less well understood signaling and developmental roles in eukaryotes (*4*−*6*). They are implicated in disease states such as diabetes mellitus (*7*). In addition, they have roles associated with cell−cell interactions as illustrated by human vascular adhesion protein (hVAP). This protein, which displays all the features of a copper amine oxidase including the conserved catalytic residues, mediates interactions between lymphocytes and endothelial cells and is important in the inflammatory response (*8*, *9*).

CuAOs are homodimers of around 160 kDa (Figure 1A) with each subunit containing one copper ion and an organic

[†] This work was supported by grants from the U.K. Biotechnology and Biological Sciences Research Council (BBSRC) and the Engineering and Physical Sciences Research Council (EPSRC) to P.F.K., S.E.V.P., and M.J.M. S.E.V.P. held an International Research Scholar award from the Howard Hughes Medical Institute. J.M.M. and C.R.K. were supported by BBSRC studentships.

[‡] File Name for Brookhaven Protein Structure Data Bank entries: Y369F variant, 1JRQ.

* To whom correspondence should be addressed. Telephone: +44 113 2332595. Fax: +44 113 233 3144. E-mail: m.j.mcpherson@leeds.ac.uk.

[§] Present address: Department of Molecular Biophysics and Biochemistry, Yale University, New Haven, CT.

[||] Present address: Department of Biochemistry, Adrian Building, University of Leicester, University Road, Leicester LE1 7RH, U.K.

[⊥] Present address: Department of Biochemistry, Molecular Biology and Biophysics, University of Minnesota, 6-155 Jackson Hall, 321 Church St. SE, Minneapolis, MN 55455.

[1] Abbreviations: TPQ, 2,4,5-trihydroxyphenylalanine quinone; CuAO, copper-containing amine oxidase; ECAO, *Escherichia coli* amine oxidase; PSAO, pea seedling amine oxidase; AGAO, *Arthrobacter globiformis* amine oxidase; HPAO, *Hansenula polymorpha* amine oxidase; 2-HP, 2-hydrazinopyridine.

10.1021/bi011187p CCC: $20.00 
Published on Web 09/29/2001

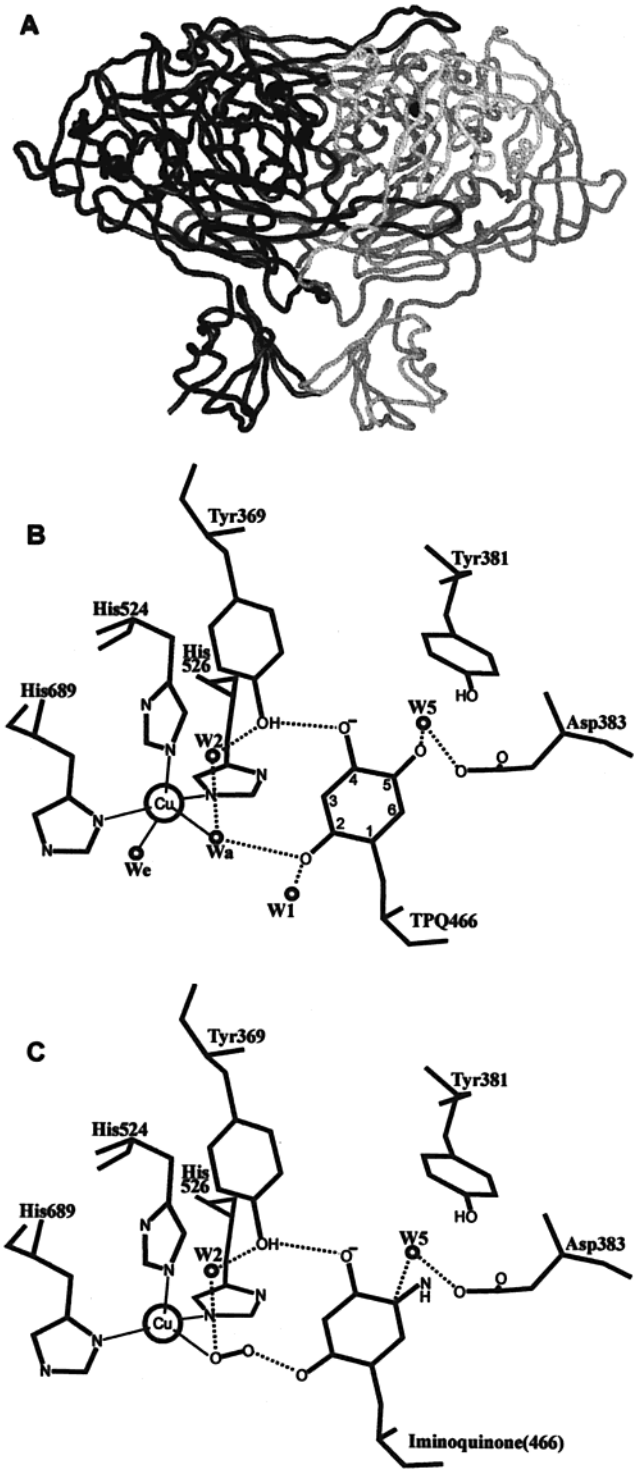


FIGURE 1: Wild-type *E. coli* copper amine oxidase structure. (A) Cα backbone diagram of the ECAO homodimer with one monomer colored black and the other gray. (B) ECAO active site showing the copper ligands (solid lines) including the axial (Wa) and equatorial (We) waters, the hydrogen bond network (dashed lines), and the TPQ with carbon atom numbering shown. (C) ECAO active site in an equilibrium turnover species illustrating features of the oxidative half-reaction (*47*) with dashed lines indicating key interactions and possible proton transfer pathways. Figure produced using SPOCK (*66*).

cofactor, 2,4,5-trihydroxyphenylalanine quinone (TPQ) (*10*). The TPQ is posttranslationally derived by a single turnover, copper- and oxygen-dependent, processing event of an active site tyrosine residue (*11*−*20*). The X-ray crystal structure of *Escherichia coli* copper amine oxidase (ECAO) (*21*) has provided important insights into the active site structure and catalytic mechanism of the copper amine oxidases. It also facilitated X-ray crystal structure determinations of CuAOs from pea seedling (PSAO) (*22*), *Arthrobacter globiformis* (AGAO) (*17*) and *Hansenula polymorpha* (HPAO) (*23*). The structures reveal a high degree of structural similarity despite low sequence identity. An amino acid sequence alignment of 14 CuAOs identified only 33 conserved residues (*24*). Each subunit of ECAO comprises four distinct domains: an N-terminal domain, which is not present in all CuAOs, two conserved domains with a cystatin-like fold, and a large β-sandwich domain (Figure 1A) containing the active site. Copper coordination is approximately square pyramidal with three His residues (His524, His526, His689) and two waters; one axial (Wa) and one equatorial (We) (Figure 1B). The TPQ is not directly liganded to the $Cu^{2+}$ and has rotational freedom with the major conformation involving a hydrogen bond between O2 of TPQ and Wa. TPQ O4 is hydrogen bonded to the hydroxyl group of Tyr369 while O5 of TPQ is directed toward the substrate binding pocket close to the conserved catalytic base Asp383 (Figure 1B). Two β-hairpins extend from one subunit to the other. One of these strands contributes residues that lie close to the active site of the other subunit, perhaps playing a role in intersubunit communication.

Enzymes isolated from different sources display substrate specificity differences and variability in the stereochemistry of proton abstraction (*25*−*34*). ECAO oxidizes aromatic primary amines such as β-phenylethylamine most efficiently (*35*); features of the reductive and oxidative half-reactions and intermediates in the catalytic mechanism of amine oxidases are shown in Figure 2.

Our understanding of the reaction mechanism of CuAOs is extensively informed by the pioneering work of Petterson and co-workers (*36*, *37*) and Klinman and colleagues (*38*−*40*). In the reductive half-cycle optimal interaction occurs between protonated substrate and enzyme with a deprotonated active site base. Substrate amine is deprotonated by the active site base (*41*, *42*) that then acts as a general acid to eliminate TPQ O5 as water to facilitate formation of a substrate Schiff base at the C-5 position of TPQ (Figure 2, steps 1 and 2). The base subsequently abstracts the C−H proton from the methylene group of the substrate Schiff base, yielding the product Schiff base by way of a carbanionic intermediate (Figure 2, step 3). Hydrolysis of the product Schiff base yields the aminoquinol form of the TPQ with release of product aldehyde (Figure 2, step 4). Studies on ECAO provided strong evidence that Asp383 is the active site base and that it has multiple roles during catalysis including stabilizing the TPQ conformation, assisting substrate binding to TPQ, and abstracting the C−H proton from substrate (*33*, *43*).

The oxidative half-cycle, involving binding of molecular oxygen and reoxidation of TPQ with release of hydrogen peroxide (step 5) and ammonia (step 6), is relatively poorly understood in comparison with the reductive half-cycle. The aminoquinol/$Cu^{2+}$ is in equilibrium with a semiquinone/$Cu^{+}$ radical species (*44*, *45*). Dioxygen is reduced, leading to formation of hydrogen peroxide and an iminoquinone state from which TPQ is regenerated by hydrolysis to release ammonia. It has recently been proposed that in bovine serum

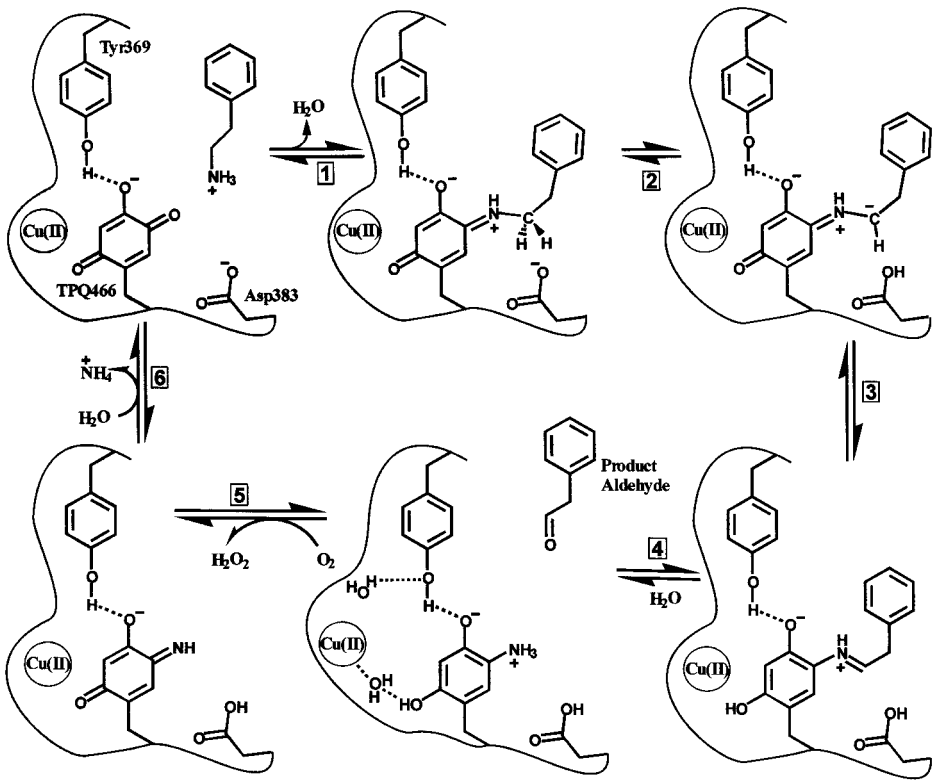


FIGURE 2: Pathway for the catalytic cycle of *E. coli* copper amine oxidase. The TPQ is shown together with the active site base, Asp383, and the conserved Tyr369. The substrate is deprotonated and forms the substrate Schiff base (step 1). A hydrogen is abstracted, by Asp383, from the methylene group (step 2), allowing rearrangement to the product Schiff base (step 3). Product aldehyde is released by hydrolysis to leave reduced enzyme (step 4); some hydrogen bonds associated with the reduced (aminoquinol) TPQ are shown by dashed lines. Oxygen, the second substrate, binds to the enzyme and is reduced to hydrogen peroxide (step 5), giving iminoquinone with subsequent hydrolysis and release of ammonia, regenerating the active enzyme (step 6).

CuAO (BSAO) the rate-determining step during the oxidative half-reaction is the first electron transfer from aminoquinol to dioxygen (*46*). This study, together with a recent cryo-crystallographic investigation of intermediates and small molecule complexes, including an aerobic turnover species of ECAO (*47*), provides a view of the interaction and communication network between components of the active site including dioxygen bridging between copper and the reduced TPQ (Figure 1C).

A conserved tyrosine (Tyr369) appears to play a central role in anchoring the position of the TPQ via a short hydrogen bond to O4 and is also implicated in proton transfer from TPQ to dioxygen (Figure 1C) (*47*). The likely importance of this residue is indicated by the reduced activity, altered substrate specificity, and reduced rate of cofactor biogenesis observed when the corresponding residue (Tyr305) was mutated in HPAO (*48*). Here we explore the role of Tyr369 in ECAO by comparative structural, kinetic, and spectral studies of the wild-type enzyme with the Y369F variant.

## EXPERIMENTAL PROCEDURES

*Mutagenesis of Tyr369, Protein Expression, and Purification.* The *ecao* gene was mutated by the PCR megaprimer method (*49*) with *Pwo* DNA polymerase (Boehringher Mannheim). PCR amplification with 100 pmol of both the M13 reverse primer and Y369F mutagenic primer and 100 ng of pAlt*ecao*-1 as template (*33*) was performed for 20 cycles (94 °C for 1 min, 55 °C for 1 min, and 72 °C for 2 min) in an MJR PTC-100 thermal cycler. A 100 ng aliquot of the gel-purified PCR megaprimer product, 100 pmol of M13(-20) and 100 ng of pAlt*ecao*-1 template restricted at the *Bgl*II site to prevent amplification of the wild-type gene (*50*), was included in a similar PCR amplification except at an annealing temperature of 52 °C. The PCR product was gel purified.

The mutagenic oligonucleotide was 5′-GCATGATTGT-GCCTT***T***CGG**G**GATCCTAGTATTG-3′ with the mutation to alter the Tyr369 codon shown in bold italics and the mutated codon overscored. A silent mutation to introduce a *Bam*HI restriction site (underscored) is in bold. The gene was cloned into the *E. coli* expression vector pKK233-3 (Amersham-Pharmacia), and a positive clone designated pKK*ecao*-Y369F was identified by *Bam*HI digestion. The DNA sequence of both strands of the mutant genes was confirmed by dideoxynucleotide sequencing on an ABI 373 instrument (PE Biosystems).

Cells were grown in 2TY growth medium (*51*) containing 55 $\mu$M $CuSO_4$, 50 mg/mL ampicillin, and 25 mg/mL carbenicillin to an $OD_{600}$ of 0.6−0.7. Protein expression was induced by adding isopropyl $\beta$-D-thiogalactopyranoside (IPTG; Melford Laboratories Ltd.) to a final concentration of 3.5 mM and allowing growth to continue for a further 4 h. ECAO wild type and Y369F were purified from a periplasmic fraction (*21*, *33*) by exploiting its characteristic affinity for Q-Sepharose high-performance media at pH 7.2. The column was equilibrated with 20 column volumes of 20 mM Tris-HCl, pH 7.2, at 5 mL/min. Concentrated protein was loaded, and the column was washed with 20 column volumes of the same buffer at 2 mL/min. ECAO was eluted

Table 1: Data Collection, Processing, and Refinement Statistics for ECAO Y369F

| | |
|---|---|
| $\lambda$ (Å) | 0.899 |
| $d_{min}$ (Å) | 2.1 |
| space group | $P2_12_12_1$ |
| unit cell dimensions *a*, *b*, *c* (Å) | 134.54, 166.45, 79.38 |
| unique reflections | 90148 |
| multiplicity (%) | 2.6 |
| completeness (%) (final shell) | 91.4 |
| $I/\sigma I$ (final shell) | 13.0 (2.3) |
| $R_{sym}$ (%) (final shell) | 4.9 (33.6) |
| resolution range (Å) | 20−2.1 |
| no. of reflections in working set | 87056 |
| no. of reflections in $R_{free}$ set | 3092 |
| non-hydrogen atoms | |
| amino acid residues | 1440 |
| protein atoms | 11352 |
| solvent molecules | 1393 |
| $Cu^{2+}$ ions | 2 |
| $Ca^{2+}$ ions | 4 |
| $R_{cryst}$ (%) | 19.5 |
| $R_{free}$ (%)[c] | 23.5 |
| average *B*-factors | |
| protein atoms (Å$^2$) | 29.8 |
| water molecules (Å$^2$) | 40.9 |
| RMSD from ideal geometry | |
| bonds (Å) | 0.010 |
| angles (deg) | 3.0 |
| Ramachandran plot | |
| energetically favored regions (%) | 88.7 |
| additionally allowed regions (%) | 10.8 |
| generously allowed regions (%) | 0.5 |
| disallowed regions (%) | 0.0 |
| RMS distance of Cα atoms of variants onto wild type (Å) | |
| A subunit | 0.17 |
| B subunit | 0.21 |

at 2 mL/min by applying a gradient of 0−350 mM NaCl in 20 mM Tris-HCl, pH 7.2. ECAO typically eluted as a broad peak at ~63 mM NaCl. Fractions were analyzed for purity by 10% SDS−PAGE, and activity assays were conducted using the coupled assay in a microtiter plate (Falcon). Pooled and concentrated fractions were subjected to gel filtration using Sephacryl HR-200 media (Amersham Pharmacia Biotech) packed into a Bio-Rad Econo column (diameter 6 cm, length 120 cm, void volume 60 mL) and equilibrated with 20 mM Tris-HCl, pH 7.2, using a flow rate of 5 mL/h. Typically, ECAO eluted after 10 h. Purity was checked by 10% SDS−PAGE and electrospray mass spectrometry, and activity was measured by the coupled assay (*21*).

*X-ray Crystallographic Data Collection and Structure Determination.* Crystals of the Y369F protein were grown from 1.26 M sodium citrate and 100 mM HEPES, pH 7.0, at 18 °C using the sitting drop vapor diffusion method. They were transferred briefly to a cryoprotectant solution containing 20% glycerol before flash cooling to 100 K in a cold nitrogen gas stream. Diffraction data were collected at 100 K using the Daresbury SRS (Synchrotron Radiation Source) with 300 mm MAR imaging plate detectors. The diffraction patterns were markedly anisotropic, with diffraction extending further in the *a*- and *b*-axis directions than along the *c*-axis, as noted previously for frozen ECAO crystals (*33*). Programs from the CCP4 suite (*52*) and DENZO (*53*) were used to process the data. Details of crystal parameters, data collection, and processing statistics are shown in Table 1. The crystal structure of Y369F was determined by cryo-crystallography as previously described for wild-type ECAO by Murray et al. (*43*).

*Mass Spectroscopy.* Samples were analyzed by inductively coupled plasma mass spectrometry (ICP-MS) using a Platform ICP instrument (Micromass U.K. Ltd., Manchester, U.K.) as described previously (*43*). For electrospray mass spectrometry protein samples were diluted in sterile deionized water to a final concentration of ~0.5 mg/mL. The samples were dialyzed overnight against ~5000 volumes of deionized water to remove any salt or unreacted inhibitor. Samples were treated in 0.05% formic acid (pH 2.0) prior to analysis on a Q-Tof instrument (Micromass U.K. Ltd., Manchester, U.K.) to provide molecular mass information.

*Enzyme Preparations for Solution Studies.* Enzyme concentration, typically in the range $(1.0-6.0) \times 10^{-6}$ M, was determined from absorbance at 280 nm adjusted by a gravimetrically derived correction factor of 0.76 to give concentration in mg mL$^{-1}$ ($\epsilon = 2.1 \times 10^5$ M$^{-1}$ cm$^{-1}$) (*54*). Enzyme was dialyzed against 20 mM phosphate buffer, pH 7.0, at 4 °C and centrifuged prior to use.

*UV−Vis Spectral Studies and TPQ Titrations.* All UV−vis spectral studies were performed on a Shimadzu UV-2401PC spectrophotometer at 25.0 °C. Two methods were used for titration of wild-type ECAO and Y369F with 2-hydrazinopyridine (2-HP). For the first method, a stock solution of 2-HP was prepared at a molar concentration 10 times that of the protein. On the basis of the protein concentration of the monomers, TPQ was titrated by stepwise additions of 0.1 equiv of 2-HP. Absorbance changes were corrected for the 1% dilution of the sample at each addition. For the second method, 10 separate aliquots of protein were titrated by the addition of single aliquots of 2-HP containing from 0.1 to 1.0 equiv. In both methods the reaction was allowed to proceed until no further increase in absorbance was detected following each addition. Where necessary, a final addition of 20 equiv of 2-HP was added to ensure full titration.

*Enzyme Activity Measurements.* Enzyme activity was measured as previously described using a coupled assay with $\beta$-phenylethylamine as substrate (*21*) in either air-saturated or oxygen-saturated reagents in solution or in crystals (*47*). Pre-steady-state measurements were made using an Applied Photophysics SX-17MV stopped-flow rapid reaction spectrophotometer essentially by following the procedure of Steinebach and colleagues (*55*, *56*). Briefly, for anaerobic experiments, all reagents were purged of oxygen under argon and transferred to an anaerobic glovebox (Belle Technology) under nitrogen atmosphere purged of oxygen to <10 ppm using catalytic deoxygenators. Reactions were performed in 100 mM sodium phosphate buffer (pH 7.0) at 25 °C with enzymes diluted to a final concentration of 5 $\mu$M in the assay mix. Substrate was present at 50 $\mu$M (>30$K_M$), rather than the 198 $\mu$M used by de Vries et al. (*56*), to minimize substrate inhibition. A reference scan was taken of assay reagents minus protein. The absorbance changes of samples containing protein were then recorded at the $\lambda_{max}$ over 0.1 s to determine an optimal time period for data collection: 10 ms for wild-type ECAO and 100 ms for Y369F.

## RESULTS

*Protein Purification and Initial Analysis.* The Y369F protein was purified as for wild type and migrated in a similar

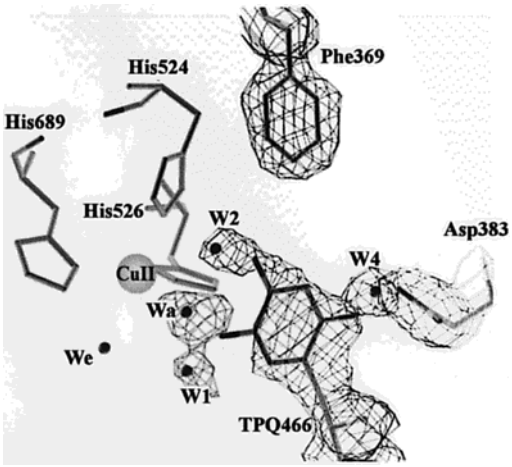


FIGURE 3: Electron density map of the active site of Y369F showing the well-defined TPQ ring.

manner during SDS−PAGE. Electrospray mass spectrometry gave a mass for wild-type ECAO of 81 286 ± 15, which is in good agreement with the predicted mass of 81 271, that includes the two additional oxygen atoms on the TPQ. The comparative difference in the ES-MS determined mass between wild type and Y369F (81 270 ± 2) of 16 corresponds to loss of the O4 atom from Tyr369.

*Crystal Structure Analysis of Y369F.* The structure of Y369F was refined to a resolution of 2.1 Å. Overall, the Y369F crystal structure is essentially identical to that of the wild-type ECAO homodimer (*21*, *43*) with equivalent atoms of wild type and Y369F having an RMSD of 0.20 Å. Data collection and processing statistics are shown in Table 1. The Y369F structure exhibits good geometry and no residues in energetically disallowed regions of the Ramachandran plot (*57*). Figure 3 shows a region of the electron density map of the active site of Y369F revealing well-defined electron density for the TPQ. Both wild type and Y369F show catalytic activity in the crystals.

*Structural Comparison of Wild Type and Y369F.* A comparison of the active sites of wild type and Y369F is shown in Figure 4. Wild type and Y369F display a high level of structural similarity with the most significant differences occurring in the active site. In wild-type ECAO the TPQ side chain is located within a wedge-shaped pocket formed by the side chains of Val367, Asp383, and Asn465 that could accommodate tetrahedral intermediates in the reductive half-reaction. This conformational constraint leads to the electron density of TPQ being stronger for O2, O4, and the ring carbons from C1 to C4 but weaker for O5, C5, and C6, reflecting a degree of conformational flexibility (*43*). As shown in Figure 1B, the TPQ O2 atom makes interactions with the axial water molecule (Wa) and another crystallographically conserved water molecule, W1, over average distances of 3.0 and 2.6 Å, respectively. The O4 atom of TPQ is involved in a 2.7 Å hydrogen bond interaction with the OH group of Tyr369, and the TPQ O5 atom lies close to the catalytic base and interacts with the carboxylate group through a mobile water molecule, W5. There is a well-ordered molecule (W2) forming a hydrogen bond between OH of Tyr369 and the axial water on the copper.

The crystal structure of the Y369F variant indicates that Tyr369 influences the conformation of both TPQ and Asp383. The removal of the hydroxyl of Tyr369 allows TPQ more flexibility to adopt other conformations, with one prevalent conformation evident in the electron density (Figure 3). This dominant conformation in the resting mutant enzyme, in which the C5 and O5 atoms of TPQ are well defined, is likely analogous to that termed a "nonproductive conformation" (*58*). There is evidence in the electron density for a minor contribution from the "on-copper" conformation as observed in the original inactive ECAO wild-type structure, crystallized from ammonium sulfate, in which O4 of TPQ is coordinated to the copper (*21*).

In the Y369F nonproductive conformation, water molecules interact with polar groups of the TPQ side chain (Figure 4). The O2 atom interacts via a water molecule, W4, with a carboxylate oxygen of the catalytic base, Asp383. The O4 group of TPQ makes a hydrogen bond (2.4 Å) with the highly conserved water molecule, W2, and O5 is close to the axial water, Wa. The water molecules W2 and Wa are well defined in all crystal structures of ECAO. Tyr381, the "substrate gate" residue (*17*, *33*) adopts different conformations in wild-type and catalytic variants. In the Y369F structure, Tyr381 is 2 Å closer to the Phe369 position than it is to Tyr369 in wild-type ECAO. In this position, the phenolic ring of Tyr381 has rotated approximately 40°.

The ability of TPQ to adopt nonproductive conformations in the resting enzyme is a feature revealed by crystal structures of native CuAOs (*17*, *22*) and resonance Raman studies of active site mutants (*48*, *58*, *59*). In the case of HPAO the N404A (N465 in ECAO) and E406N (D467 in ECAO) variants appear to undergo a slow conformational change of Schiff base intermediates to a nonproductive conformation. In contrast, the Y305A (Y369 in ECAO) variant data suggest a rapid and reversible formation of a nonproductive product Schiff base. These observations indicate the importance of hydrogen-bonding interactions in maintaining productive conformations of TPQ in the resting enzyme, product Schiff base, and presumably reduced TPQ states.

*TPQ Formation.* In the work of Hevel et al. (*48*), the HPAO Y305F variant was shown to react more slowly than wild-type HPAO with phenylhydrazine and was estimated to contain around 0.3 TPQ per monomer. To investigate whether the ECAO Y369F variant behaved similarly, we have studied the TPQ content of this protein in comparison with wild-type ECAO. The presence of a significant population of TPQ in the electron density maps of Y369F and a substantial extinction coefficient of 1495 ± 36 $M^{-1}$ $cm^{-1}$ per monomer at 496 nm for Y369F compared with 1990 ± 32 $M^{-1}$ $cm^{-1}$ per monomer at 480 nm for wild type (Figure 5) suggested that Tyr369 is not essential for TPQ formation. The difference in extinction coefficient may reflect differences in the electronic state of the TPQ in wild type compared with Y369F. In addition to the red-shifted $\lambda_{max}$, the spectrum of Y369F reveals a broader peak than wild type, consistent with the lack of a hydrogen bond between TPQ and the OH of Tyr369 and differences in the electronic structure of TPQ. The lower extinction coefficient of Y369F could also reflect a reduced TPQ content, as noted for HPAO Y305F. Thus it was important to determine the TPQ content in Y369F to allow comparison with wild-type ECAO and with the Y305F variant of HPAO. Both Y369F and wild-type ECAO were titrated with 2-HP, which forms irreversible adducts with TPQ. 2-HP was preferred over the phenylhy-

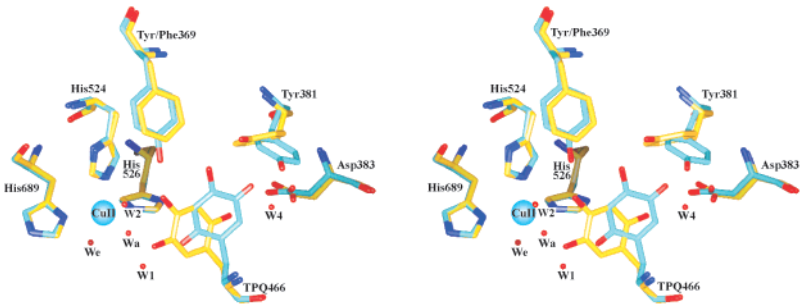


FIGURE 4: Stereoview of an overlay of the active sites of *E. coli* copper amine oxidase wild type and Y369F. In general, the structures of the resting enzyme are very similar, although the difference in TPQ conformation from productive in wild type to nonproductive in Y369F is clearly shown. The water molecules at the copper site are essentially unchanged whereas W5 associated with TPQ in wild type has been lost and a new water W4 is observed. Carbon atoms in the wild-type structure are colored cyan and in Y369F yellow. Figure produced using SPOCK (*66*).

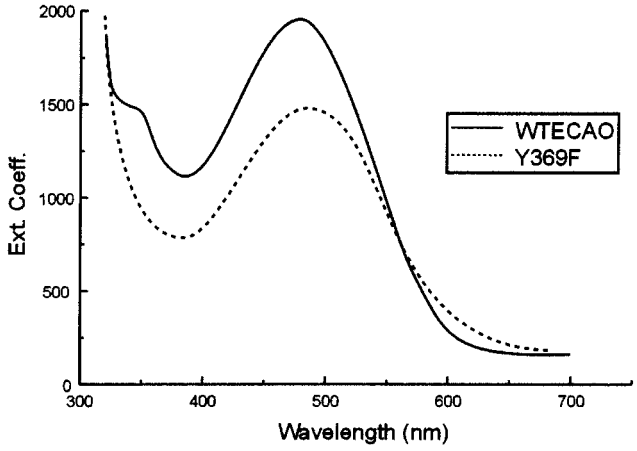


FIGURE 5: UV−vis spectra of *E. coli* copper amine oxidase wild type and Y369F.

drazine family of irreversible inhibitors because of its long-term stability. In wild type, the reaction results in the formation of an initial adduct (adduct I, $\lambda_{max}$ 420−435 nm), which is slowly converted to a second spectroscopically distinct species (adduct II, $\lambda_{max}$ 525−540 nm). Wild-type ECAO forms adduct II very slowly such that at pH 6.0 virtually no spectral changes in the 530 nm region occur, and the titration of TPQ was therefore measured at this pH by adduct I accumulation at 423 nm. In the case of Y369F at pH 6.0 both adduct I and adduct II are observed while at pH 8.0 conversion to adduct II is essentially complete. Titration of TPQ in this variant was thus performed at pH 8.0 by following absorbance at 530 nm. As the titrations of wild type and Y369F were conducted under different conditions, it is not possible to compare the rates of adduct formation recorded during these experiments. It was found that wild-type enzyme reacts rapidly with 2-HP to form adduct I until ~1.5 TPQs per dimer have been titrated. The reaction then becomes extremely slow although it can be driven to completion (2.1 ± 8% TPQ per dimer) by addition of excess 2-HP. In contrast, for Y369F, 1.95 ± 5% TPQs per dimer are titrated by 2 equiv of 2-HP without addition of excess 2-HP. The titrations were performed by two procedures (see Experimental Procedures), and the results were in excellent agreement. In addition, ES-MS was performed and revealed a predominant species in the 2-HP adduct of Y369F of 81 350 ± 5, which is 80 mass units greater than the monomer mass of the nontitrated sample. This additional mass is in reasonable agreement with the expected mass of the TPQ/2-HP adduct (+90), indicating that all of the monomers had reacted with 2-HP. For wild type the mass shift was 150, which may comprise 2-HP plus copper, perhaps reflecting a conformational difference between the adduct I and adduct II forms that influences copper retention during ES-MS.

Clearly, given the different relative amounts of adducts I and II formed under equivalent conditions within the two enzymes, the loss of the Tyr369 hydroxyl has a dramatic influence on the chemistry of adducted forms of the enzymes. The titrations reveal a more rapid formation of adduct 2 and an end point corresponding to complete TPQ content in Y369F. Importantly, these studies reveal that Tyr369 is not essential for complete TPQ formation and highlight a distinct difference between Y369F and HPAO Y305F, in which TPQ formation was reported to be incomplete.

*Kinetic Characteristics of Y369F.* Both wild type and Y369F are active in the crystals and in solution, indicating that Tyr369 is not essential for catalytic activity. We have made comparative kinetics measurements for wild-type ECAO and Y369F over a range of pH values (Table 2) and under different oxygen concentrations. Reaction rates for wild-type ECAO and Y369F under the air-saturated conditions (~250 $\mu$M) used for all other assays were identical to those conducted using oxygen-saturated (~1250 $\mu$M) buffers. This demonstrates that under our standard assay conditions the oxygen concentration is not limiting the overall rate. It is clear that despite the predominance of a nonproductive conformation in the crystal structure of the resting state this does not prevent substrate binding to the C5 of TPQ either in the crystal or in solution. The wild type and Y369F variant display closely similar $K_M$ values for $\beta$-phenylethylamine, at pH 7.0, of 1.2 and 1.5 $\mu$M, respectively (Table 2). It is the catalytic efficiency of amine oxidation that is most significantly affected in the Y369F variant. Wild-type ECAO oxidizes $\beta$-phenylethylamine at pH 7.0 with a $k_{cat}$ of 15.0 ± 0.8 $s^{-1}$ compared with 0.38 ± 0.02 $s^{-1}$ for Y369F. Thus, in Y369F, the $k_{cat}/K_M$ is reduced approximately 50-fold from $1.25 \times 10^{-7}$ $M^{-1}$ $s^{-1}$ for wild type to $0.025 \times 10^{7}$ $M^{-1}$ $s^{-1}$ for Y369F (Table 2). At the higher pH values of 7.5 and 8.0 Y369F is slightly more efficient with a 30- and 27-fold decrease in catalytic efficiency, respectively (Figure 6). The value of $k_{cat}$ for wild type reported here is correct, although it is 8-fold lower than we have previously reported (*43*).

The plot of $k_{cat}/K_M$ for $\beta$-phenylethylamine vs pH is approximately bell shaped for wild type, with a p$K_a$ ≈5.75

Table 2: Relative Rates for $\beta$-phenylethylamine Oxidation by Wild-type ECAO and Y369F at a Range of pH Values

| | wild-type ECAO | | | Y369F | | | |
|---|---|---|---|---|---|---|---|
| pH | $k_{cat}$ ($s^{-1}$) | $K_M$ ($\mu$M) | $k_{cat}/K_M$ ($M^{-1}s^{-1}$) $\times 10^6$ | $k_{cat}$ ($s^{-1}$) | $K_M$ ($\mu$M) | $k_{cat}/K_M$ ($M^{-1}s^{-1}$) $\times 10^6$ | ratio $k_{cat}/K_M$ wild type:Y369F |
| 5.5 | $9.4 \pm 0.6$ | $7.8 \pm 0.4$ | $1.2 \pm 0.1$ | $0.28 \pm 0.02$ | $5.9 \pm 0.5$ | $0.05 \pm 0.01$ | 24 |
| 5.75 | $11.1 \pm 0.7$ | $2.3 \pm 0.1$ | $4.8 \pm 0.6$ | $0.44 \pm 0.01$ | $6.1 \pm 0.2$ | $0.07 \pm 0.01$ | 69 |
| 6.0 | $20.3 \pm 0.7$ | $1.8 \pm 0.1$ | $11.3 \pm 1.1$ | $0.48 \pm 0.03$ | $6.1 \pm 0.4$ | $0.08 \pm 0.01$ | 141 |
| 6.5 | $19.4 \pm 0.8$ | $1.7 \pm 0.1$ | $11.4 \pm 1.2$ | $0.39 \pm 0.01$ | $2.4 \pm 0.1$ | $0.16 \pm 0.01$ | 71 |
| 7.0 | $15.0 \pm 0.8$ | $1.2 \pm 0.1$ | $12.5 \pm 1.9$ | $0.38 \pm 0.02$ | $1.5 \pm 0.1$ | $0.25 \pm 0.04$ | 50 |
| 7.5 | $14.1 \pm 0.6$ | $1.7 \pm 0.2$ | $8.3 \pm 1.5$ | $0.36 \pm 0.01$ | $1.3 \pm 0.1$ | $0.27 \pm 0.04$ | 31 |
| 8.0 | $12.9 \pm 0.2$ | $2.3 \pm 0.1$ | $5.6 \pm 0.4$ | $0.19 \pm 0.01$ | $0.9 \pm 0.1$ | $0.21 \pm 0.04$ | 27 |

and a basic p$K_a$ above 8.0, which are attributed to the catalytic base and substrate, respectively (Figure 6). The corresponding plot for Y369F is also bell shaped but with a shift in the lower p$K_a$ to ≈6.5 and with a basic p$K_a$ again above 8.0. Wild-type ECAO displays the highest $k_{cat}/K_M$ value at pH 6.75 while for Y369F the optimal pH is 7.3. In contrast with wild type, Y369F begins to show a significant reduction in catalytic efficiency below pH 6.5. This reduction is due to an effect on $K_M$ rather than $k_{cat}$ probably due to a perturbed p$K_a$ of the catalytic base Asp383. Alteration of the protonation state of Asp383 in Y369F could affect optimal interaction with the protonated substrate, thereby reducing the efficiency of substrate binding.

*Transient Kinetics.* It is well established that reduction of TPQ by substrate leads to loss of absorption in the 480−500 nm range (*36*, *56*, *60*, *61*) although this has not been ascribed to a particular step in the reductive half-reaction. As a preliminary approach to identifying the rate-limiting step in the Y369F variant, we measured substrate reduction by following the loss of TPQ absorbance using stopped-flow rapid reaction spectrophotometry. Initial experiments were conducted under relatively strict anaerobic conditions, but later repetition under aerobic conditions gave identical results as anticipated for an initial oxygen-independent step in the reductive half-reaction. The "dead time" of the spectrophotometer was 1.5 ms before recording started. Figure 7 indicates that the rate constant (taken to be first order) for decay of absorbance at 487 nm by $t_{1/2}$ is 935 $s^{-1}$ for wild type and 63 $s^{-1}$ for Y369F. There is also a lag before loss of the absorbance in both wild type and Y369F, with the duration of this lag being some 10-fold longer in the mutant. While we cannot ascribe these events to specific stages in the reductive half-reaction, it is clear that they are not rate limiting for either wild-type ECAO or Y369F that display $k_{cat}$ values at pH 7.0 of 15 $s^{-1}$ or 0.38 $s^{-1}$, respectively.

*Metal Analysis by Mass Spectrometry.* The metal analyses averaged over both copper isotopes revealed 2.8 Cu per dimer for wild-type ECAO and 2.6 Cu per dimer for Y369F. There was no detectable zinc. These values indicate complete copper loading.

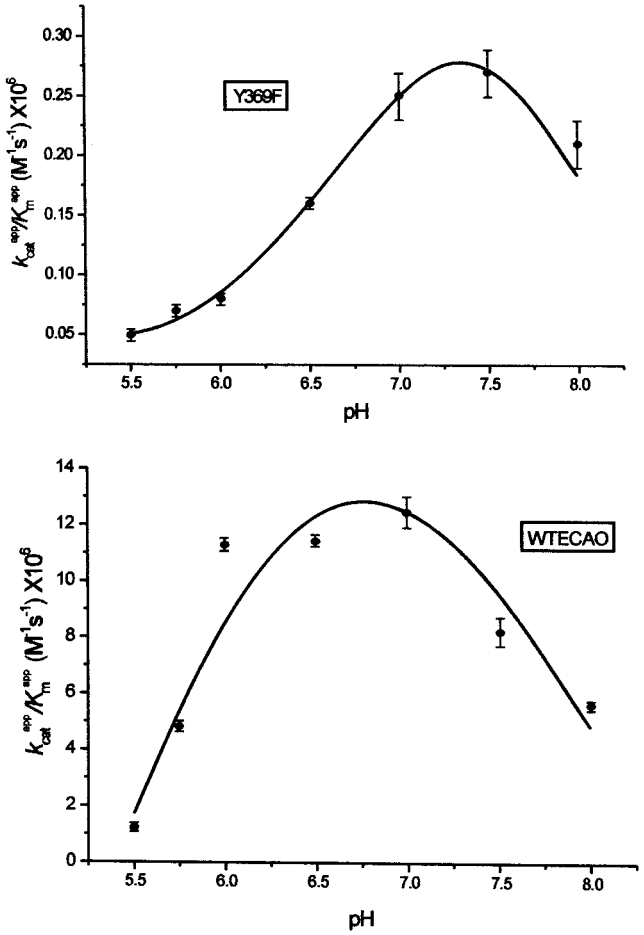


FIGURE 6: pH profiles of the catalytic efficiency of *E. coli* copper amine oxidase wild type and Y369F shown as $k_{cat}/K_M$ over the pH range 5.5−8.0.

## DISCUSSION

The present study on the effect of mutating a conserved tyrosine residue in the active site of ECAO reveals that Tyr369 is not mandatory for either TPQ biogenesis or catalytic activity.

Measurement of TPQ content indicates that, in both wild-type ECAO and Y369F, TPQ reacts with 1 equiv of 2-HP per monomer. Our experiments do not allow any assessment of variation in the rate of TPQ formation. There is a significant difference in the mode of reaction of 2-HP with Y369F compared with wild type, and quantitation of the TPQ

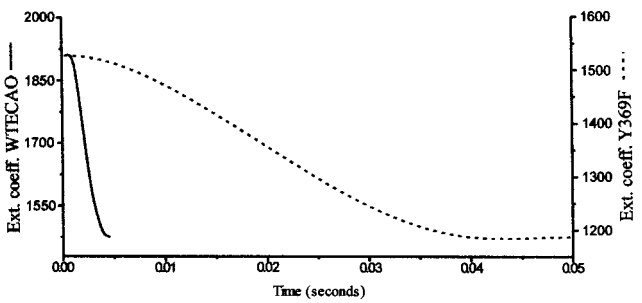


FIGURE 7: Transient kinetics data on *E. coli* copper amine oxidase wild type and Y369F. Rapid reaction spectra were recorded at 487 nm to monitor the disappearance of the oxidized TPQ species.

stoichiometry in the two proteins required measurements under different reaction conditions. For this reason we are unable to compare the rates of reaction of 2-HP with wild-type ECAO and Y369F. It is of interest that for wild type 1.5 TPQs per dimer are readily titratable in a quantitative manner, and the remainder reacts only following addition of excess 2-HP. This implies that a population of TPQs is not so readily capable of interaction with 2-HP because they are either initially chemically distinct or inaccessible. In CuAOs there are long $\beta$-strands that extend from the active site of one monomer to the active site of the other monomer, providing a potential mechanism for communication between active sites (Figure 1A). It seems possible that, at least in some CuAOs, the reaction of 2-HP with the TPQ in one subunit of a dimer may influence the reactivity of the TPQ in the second subunit. This aspect of CuAOs and the role of any intersubunit communication mechanism require further study.

In ECAO, at pH 7.0, Y369F shows a slight increase in $K_M$ for $\beta$-phenylethylamine, from 1.2 to 1.5 $\mu$M, with a more substantial effect on $k_{cat}$, showing a 39-fold decrease from 15.0 to 0.38 $s^{-1}$. These differences in kinetic parameters, however, result in only a 50-fold reduction in $k_{cat}/K_M$, indicating that while Tyr369 plays a role in catalysis, this role is not essential. The altered behavior of the Y369F variant over the pH range studied (5.5−8.0), particularly at pH 6.5 and below, reveals an increase in p$K_a$ of the catalytic base, consistent with an altered active site environment. We have also shown by transient kinetics measurements that early events in the reductive half-reaction are affected by the mutation, although these do not represent the rate-limiting step.

The identities of the intermediates formed in the reductive half-cycle remain unclear. Previous stopped-flow studies on anaerobic reduction of wild-type ECAO by $\beta$-phenylethylamine were unable to follow loss of the TPQ species due to the 6 ms dead time of their instrument (*55*, *56*). An intermediate with $\lambda_{max}$ 400 nm, which was observed in a difference spectrum, was assigned as the protonated product Schiff base. This assignment was based on the similarity of the spectral properties of the 400 nm species with those of a synthesized model compound (*62*). The model compound studies, however, mimicked the reaction of TPQ with benzylamine, resulting in a compound containing a fully conjugated ring system. The spectral properties of the analogous protonated product Schiff base formed with $\beta$-phenylethylamine (*55*, *56*) are unlikely to be similar, since its ring system would not be conjugated. More detailed studies to characterize reaction intermediates are required, and the Y369F variant, which displays slower rates of reaction, may prove a useful tool in this regard.

Although Tyr369 is not an essential residue, it seems likely, from the present studies of the effects of the Y369F mutation, that this residue influences multiple stages of the catalytic cycle including an effect on the rate-limiting step. X-ray structural information provides an important basis for understanding the molecular basis underpinning these possible roles of Tyr369. First, in Y369F the TPQ is more mobile and can adopt a nonproductive conformation in the resting state with potential effects on the initial stages of substrate binding. Second, the chemical environment of TPQ in the Y369F active site is altered. This may affect the hydrogen bond network and interactions between the copper and TPQ cofactors in the active site and also perturb the p$K_a$ of the multifunctional catalytic base, Asp383. Third, from previous crystal structure analysis of catalytic intermediates of ECAO (*47*) and solution studies of BSAO (*46*), the phenolic OH of Tyr369 is implicated as part of a proton shuttle in the oxidative half-reaction. We now consider each of these possibilities in more detail.

*Productive TPQ Conformation.* The ECAO crystal structure suggests that the interaction between O4 of TPQ and OH of Tyr369 plays a role in the optimal positioning of the cofactor for reaction with substrate. In Y369F, this interaction is absent, disrupting the hydrogen bond network in the active site. On the basis of the crystal structure of Y369F, the resultant effect on TPQ is the observed high-level occupancy of a nonproductive conformation. In this orientation, the O4 atom of TPQ is hydrogen bonded to W2 at a distance of 2.4 Å (Figures 3 and 4). This interaction results in a lengthening of the distance between W2 and Wa, an axial copper ligand, from 3.0 to 3.5 Å. The orientation of TPQ in this nonproductive conformation may account for the observed ~10-fold increase in the lag during the transient phase of TPQ reduction in Y369F. In addition, conformational flexibility may also reduce the time that TPQ occupies optimal orientations throughout catalysis, perhaps accounting for the observed slower rate of loss of the oxidized TPQ species during reduction (Figure 7).

It has been observed in the HPAO variants, E406N (*58*), N404A (*59*), and Y305A (*48*), that, with the preferred substrate methylamine, the cofactor appears able to adopt conformations, in a pH-dependent manner, that inhibit enzyme activity. Above pH 7.0, the product Schiff base is proposed to ionize and flip into a nonproductive conformation (*48*). However, with the larger substrate ethylamine this feature was not observed. It seems likely that for the larger ethylamine-derived product Schiff base there is insufficient space for a flip into the nonproductive conformation. For ECAO, with $\beta$-phenylethylamine as the preferred substrate, $k_{cat}/K_M$ vs pH profiles for wild-type ECAO and Y369F are similar above pH 7.0, and we would anticipate that the Phe369 ring would prevent flipping of the large phenylethylamine product Schiff base, consistent with the reasonable catalytic rate in the variant. It seems likely, however, as suggested by Hevel et al. (*48*), that TPQ, aminoquinol, and iminoquinone may be capable of rapid conformational change. The evidence from Y369F suggests the importance of the TPQ O4 and Tyr369 OH hydrogen bond for maintaining the predominant productive conformation of TPQ and, by implication, of aminoquinone and iminoquinone. Nonetheless, given the increased flexibility in the Y369F active site, we cannot rule out the possibility of a reversible nonproductive Schiff base species as observed for the HPAO Y305A variant.

*Altered Active Site Environment and the Catalytic Base.* The environment of Asp383 is altered as indicated by the increased p$K_a$ in Y369F leading to a narrower range of pH over which the variant is maximally active. Thus at pH 6.0, $k_{cat}/K_M$ of Y369F is 140-fold lower than wild-type ECAO compared with only 50-fold at pH 7.0. The UV−vis spectrum of Y369F differs from wild type with a red-shifted $\lambda_{max}$ of 496 nm compared with 480 nm and a broader peak profile. Such differences reflect alterations in the electronic structure

of the TPQ, presumably due to the loss of the hydrogen bond between O4 and Tyr369 OH affecting charge localization at C4.

The importance of the hydrogen bond between TPQ O4 and Tyr369 OH for the stabilization of catalytic intermediates is demonstrated by the structure of ECAO with 2-hydrazinopyridine (2-HP) bound (*33*). The 2-HP structure is analogous to the substrate Schiff base and therefore provides insight into the interactions between active site residues and this intermediate. Reductive trapping experiments have indicated that the substrate Schiff base intermediate has a $\lambda_{max} = 340$ nm (*63*). Spectroscopic characterization of adducts of amines with model TPQ compounds indicates that the substrate Schiff base complex has considerable *p*-quinone structure with increased charge localization on the TPQ O4, in contrast to the resting state where there is considerable charge delocalization between the O2 and O4 oxygen atoms. The charge localization in the substrate Schiff base complex has been proposed to occur through an electrostatic interaction (*64*). The ECAO−2-HP complex shows that this charge localization is likely to occur through the 2.3 Å interaction between OH of Tyr369 and O4 of TPQ. This close interaction, compared to 2.7 Å in the unadducted enzyme, suggests increased charge localization at the O4 position, resulting in the sharing of a proton between this atom and the Tyr369 OH group. In the Y369F variant where such an interaction cannot occur, the substrate Schiff base would be destabilized.

*Proton Transfer*. Previous studies, most importantly those of Su and Klinman (*46*) and Wilmot et al. (*47*), have identified a potential role for the conserved tyrosine in proton transfer during the oxidative half-reaction. Detailed kinetic analysis of the oxidative half-reaction of bovine serum amine oxidase (BSAO) by UV−vis, stopped-flow, and EPR spectroscopies, effects of viscosity, $^{18}O$ kinetic isotope effects, and computer simulation concluded that the rate-limiting step in the oxidative half-cycle is the first electron transfer to oxygen (*46*). It was also indicated that both protons for reduction of $O_2$ to $H_2O_2$ are transferred from reduced TPQ, with one likely to be substrate derived (*28*) via TPQ O4 and the other from the axial water via TPQ O2 (*40*). The crystal structure determination of ECAO catalytic intermediates during aerobic turnover has provided a structural context for these kinetic studies (*47*). The rate-determining species in crystals reveals both a dioxygen species situated between the O2 of iminoquinone and copper and possible proton transfer pathways consistent with the proposals of Su and Klinman (*46*) including one involving OH of Tyr369. The two protons originate from the reduced TPQ cofactor, and the transfer pathways involved are suggested to be directly from cofactor O2 and indirectly from cofactor O4 via the hydroxyl of the conserved Tyr369 and a conserved water (W2) as shown in Figure 1C. It is therefore possible that in Y369F the efficiency of the latter proton transfer is reduced.

In terms of the postulated direct proton transfer to dioxygen from cofactor O2, the loss of Tyr369 OH does not affect the interaction of TPQ O2 with the axial water molecule or the interaction between the axial water molecule and W2. However, the distance between the axial water molecule and the copper ion is reduced from a distance of 2.9 Å in resting ECAO to 2.6 Å in the 2-HP complex. The change in the distance between the copper and the axial water precedes the rapid hydrolysis of the product Schiff base intermediate. This supports the hypothesis that the O2 of TPQ accepts a proton from the axial water in going from the product Schiff base intermediate to the aminoquinol intermediate (*40*).

While HPAO Y305F shows a 500-fold reduction in $k_{cat}/K_M$ compared to wild-type HPAO, two other mutations at this residue, Y305C and Y305A, proved more active, showing only 3.3- and 10-fold reductions in $k_{cat}/K_M$, respectively. This effect was attributed to the possibility that a water molecule could occupy a site vacated by the tyrosine ring when a residue with smaller side chain occupied the site. The presence of an additional water molecule that could affect proton transfer to dioxygen in place of the hydroxyl of Tyr is consistent with the observed $k_{cat}/K_M$ trends for these HPAO mutants. By contrast, the conservative change of Tyr to Phe would not create sufficient space for a water molecule to occupy the site of the missing O4. It seems likely that this situation will also be true for ECAO Y369F, and indeed, the crystal structure shows no evidence for a new water molecule. There are, however, clear changes in the hydrogen-bonding pattern of TPQ that may affect the rate of proton transfer to oxygen. If Tyr369 OH plays a role in proton transfer, then the 50- and 500-fold reductions in $k_{cat}/K_M$ for ECAO Y369F and HPAO Y305F, respectively, imply that a Tyr369 OH mediated proton transfer pathway is less critical in ECAO than in HPAO.

On the basis of the present studies the conclusion that Y369F is not essential for TPQ formation or catalytic activity is in general agreement with those of Hevel et al. (*48*), who investigated mutations of the corresponding residue Tyr305 in HPAO. However, for ECAO Y369F titration with 2-HP shows one TPQ per monomer compared with impaired levels of 0.3−0.7 TPQ per monomer reported in the HPAO variants Y305F and Y305A, respectively. Differences are also revealed between HPAO Y305F and ECAO Y369F in their kinetic parameters. At pH 7.0 for HPAO Y305F, the $K_M$ for ethylamine is increased from 0.38 to 1.6 mM, a 4-fold effect, with $k_{cat}$ reduced by 125-fold from 20 to 0.16 $s^{-1}$, leading to a 500-fold decrease in $k_{cat}/K_M$. In contrast, Y369F shows only a 50-fold decrease in $k_{cat}/K_M$.

These differences in TPQ content and catalytic rate suggest that despite overall structural similarity there is significant functional variance in the active sites of CuAOs. Previous studies on the catalytic base in these two enzymes (*43*, *65*) also revealed variation in catalytic properties conferred by equivalent mutations. This presumably reflects the relative abilities of the active site residues or waters to compensate for the mutations during TPQ biogenesis and catalysis, including the productive accommodation of catalytic intermediates.

*Conclusions.* Structural analysis has demonstrated that the Tyr369 O4 is important for maintaining TPQ in a conformation that is likely to facilitate catalysis. Removal of this atom allows TPQ to adopt a nonproductive conformation in the resting enzyme. The effects of the observed increase in conformational flexibility of TPQ in Y369F, and that proposed in equivalent HPAO mutants, may account for the reduced catalytic efficiency of these variants. Kinetic studies using $\beta$-phenylethylamine as substrate indicate that $k_{cat}$ rather than $K_M$ is the parameter predominantly affected in Y369F at pH 7.0 and above. It remains to be resolved whether the

rate-limiting step occurs in the reductive or oxidative half-reaction, although it has been shown that it does not occur during the initial stages of the reductive half-reaction. The hydrogen bond network in wild type suggests that the Tyr369 O4 group could serve as a component of a proton shuttle for the substrate-derived proton that reduces copper-bound oxygen to $H_2O_2$. However, the substantial activity retained in the Y369F enzyme indicates that either Tyr369 does not participate in this proton shuttle or the Y369F active site is able to compensate for loss of this hydrogen bond network component. Mutation of the homologous residue, Tyr305, in HPAO has revealed a role in substrate specificity, cofactor biogenesis, and catalysis compared with mutation of Tyr369 in ECAO that appears to affect catalysis. The differences in properties of the equivalent mutants ECAO Y369F and Y305F indicate that apparently similar active sites display subtle differences in residue reactivity and function. Further studies are underway to define the rate-limiting step in ECAO Y369F and to identify further reaction intermediates by cryocrystallography.

## ACKNOWLEDGMENT

We thank Sarah Deacon for technical assistance, Dr. A. Ashcroft for performing the ES-MS experiments, and Micromass U.K. Ltd., Manchester, U.K., for the metal analyses using ICP-MS. We are grateful to Dr. Malcolm Halcrow for helpful discussions.

## REFERENCES

1. Parrott, S., Jones, S., and Cooper, R. A. (1987) *J. Gen. Microbiol. 133*, 347−351.
2. Cooper, R. A., Knowles, P. F., Brown, D. E., McGuirl, M. A., and Dooley, D. M. (1992) *Biochem. J. 288*, 337−340.
3. Hacisalihoglu, A., Jongejan, J. A., and Duine, J. A. (1997) *Microbiology 143*, 505−512.
4. Callingham, B. A., Crosbie, A. E., and Rous, B. A. (1995) *Prog. Brain Res. 106*, 305−321.
5. McIntire, W. S. (1998) *Annu. Rev. Nutr. 18*, 145−177.
6. Moller, S. G., and McPherson, M. J. (1998) *Plant J. 13*, 781−791.
7. Boomsma, F., vanVeldhuisen, D. J., deKam, P. J., ManintVeld, A. J., Mosterd, A., Lie, K. I., and Schalekamp, M. (1997) *Cardiovasc. Res. 33*, 387−391.
8. Bono, P., Salmi, M., Smith, D. J., and Jalkanen, S. (1998) *J. Immunol. 160*, 5563−5571.
9. Smith, D. J., Salmi, M., Bono, P., Hellman, J., Leu, T., and Jalkanen, S. (1998) *J. Exp. Med. 188*, 17−27.
10. Janes, S. M., Mu, D., Wemmer, D., Smith, A. J., Kaur, S., Maltby, D., Burlingame, A. L., and Klinman, J. P. (1990) *Science 248*, 981−987.
11. Cai, D., and Klinman, J. P. (1994) *J. Biol. Chem. 269*, 32039−32042.
12. Hanlon, S. P., Carpenter, K., Hassan, A., and Cooper, R. A. (1995) *Biochem. J. 306*, 627−630.
13. Tanizawa, K. (1995) *J. Biochem. (Tokyo) 118*, 671−678.
14. Nakamura, N., Matsuzaki, R., Choi, Y. H., Tanizawa, K., and Sanders-Loehr, J. (1996) *J. Biol. Chem. 271*, 4718−4724.
15. Cai, D. Y., Williams, N. K., and Klinman, J. P. (1997) *J. Biol. Chem. 272*, 19277−19281.
16. Ruggiero, C. E., Smith, J. A., Tanizawa, K., and Dooley, D. M. (1997) *Biochemistry 36*, 1953−1959.
17. Wilce, M. C., Dooley, D. M., Freeman, H. C., Guss, J. M., Matsunami, H., McIntire, W. S., Ruggiero, C. E., Tanizawa, K., and Yamaguchi, H. (1997) *Biochemistry 36*, 16116−16133.
18. Dooley, D. M., Bollinger, J., McGuirl, M., Ruggiero, C., and Rogers, M. (1999) *J. Inorg. Biochem. 74*, 21.
19. Dove, J. E., Schwartz, B., Williams, N. K., and Klinman, J. P. (2000) *Biochemistry 39*, 3690−3698.
20. Schwartz, B., Dove, J. E., and Klinman, J. P. (2000) *Biochemistry 39*, 3699−3707.
21. Parsons, M. R., Convery, M. A., Wilmot, C. M., Yadav, K. D., Blakeley, V., Corner, A. S., Phillips, S. E., McPherson, M. J., and Knowles, P. F. (1995) *Structure 3*, 1171−1184.
22. Kumar, V., Dooley, D. M., Freeman, H. C., Guss, J. M., Harvey, I., McGuirl, M. A., Wilce, M. C., and Zubak, V. M. (1996) *Structure 4*, 943−955.
23. Li, R. B., Klinman, J. P., and Mathews, F. S. (1998) *Structure 6*, 293−307.
24. Tipping, A. J., and McPherson, M. J. (1995) *J. Biol. Chem. 270*, 16939−16946.
25. Boadle, M. C., and Blaschko, H. (1968) *Comp. Biochem. Physiol. 25*, 129−138.
26. Battersby, A. R., Staunton, J., Klinman, J., and Summers, M. C. (1979) *FEBS Lett. 99*, 297−298.
27. Summers, M. C., Markovic, R., and Klinman, J. P. (1979) *Biochemistry 18*, 1969−1979.
28. Farnum, M. F., and Klinman, J. P. (1986) *Biochemistry 25*, 6028−6036.
29. Pec, P., and Frebort, I. (1991) *Biochem. Int. 24*, 633−640.
30. Scaman, C. H., and Palcic, M. M. (1992) *Biochemistry 31*, 6829−6841.
31. Palcic, M. M., Scaman, C. H., and Alton, G. (1995) *Prog. Brain Res. 106*, 41−47.
32. Shah, M. A., Scaman, C. H., Palcic, M. M., and Kagan, H. M. (1993) *J. Biol. Chem. 268*, 11573−11579.
33. Wilmot, C. M., Murray, J. M., Alton, G., Parsons, M. R., Convery, M. A., Blakeley, V., Corner, A. S., Palcic, M. M., Knowles, P. F., McPherson, M. J., and Phillips, S. E. V. (1997) *Biochemistry 36*, 1608−1620.
34. Yu, P. H. (1998) *J. Neural Transm., Suppl.*, 201−216.
35. Roh, J. H., Suzuki, H., Azakami, H., Yamashita, M., Murooka, Y., and Kumagai, H. (1994) *Biosci., Biotechnol., Biochem. 58*, 1652−1656.
36. Lindstrom, A., Olsson, B., Olsson, J., and Pettersson, G. (1976) *Eur. J. Biochem. 64*, 321−326.
37. Lindstrom, A., and Pettersson, G. (1978) *Eur. J. Biochem. 84*, 479−485.
38. Klinman, J. P., and Mu, D. (1994) *Annu. Rev. Biochem. 63*, 299−344.
39. Klinman, J. P. (1996) *J. Biol. Chem. 271*, 27189−27192.
40. Klinman, J. P. (1996) *Chem. Rev. 96*, 2541−2561.
41. Hartmann, C., and Klinman, J. P. (1991) *Biochemistry 30*, 4605−4611.
42. Farnum, M., Palcic, M., and Klinman, J. P. (1986) *Biochemistry 25*, 1898−1904.
43. Murray, J. M., Saysell, C. G., Wilmot, C. M., Tambyrajah, W. S., Jaeger, J., Knowles, P. F., Phillips, S. E. V., and McPherson, M. J. (1999) *Biochemistry 38*, 8217−8227.
44. Dooley, D. M., McIntire, W. S., McGuirl, M. A., Cote, C. E., and Bates, J. L. (1990) *J. Am. Chem. Soc. 112*, 2782−2789.
45. Warncke, K., Babcock, G. T., Dooley, D. M., McGuirl, M. A., and McCracken, J. (1994) *J. Am. Chem. Soc. 116*, 4028−4037.
46. Su, Q. J., and Klinman, J. P. (1998) *Biochemistry 37*, 12513−12525.
47. Wilmot, C. M., Hajdu, J., McPherson, M. J., Knowles, P. F., and Phillips, S. E. V. (1999) *Science 286*, 1724−1728.
48. Hevel, J. M., Mills, S. A., and Klinman, J. P. (1999) *Biochemistry 38*, 3683−3693.
49. Sarkar, G., and Sommer, S. S. (1990) *BioTechniques 8*, 404−407.
50. Ogel, Z. B., and McPherson, M. J. (1990) *Protein Eng. 5*, 467−468.
51. Sambrook, J., Fritsch, E. F., and Maniatis, T. (1989) *Molecular Cloning*, 2nd ed., Cold Spring Harbor Laboratory Press, Cold Spring Harbor, NY.
52. Bailey, S. (1994) *Acta Crystallogr., Sect. D: Biol. Crystallogr. 50*, 760−763.

53. Otwinowski, Z., and Minor, W. (1997) *Methods Enzymol. 276*, 307−326.
54. Saysell, C. G., Murray, J. M., Wilmot, C. M., Brown, D. E., Dooley, D. M., Phillips, S. E. V., McPherson, M. J., and Knowles, P. F. (2000) *J. Mol. Catal. B: Enzym. 8*, 17−25.
55. Steinebach, V., Devries, S., and Duine, J. A. (1996) *J. Biol. Chem. 271*, 5580−5588.
56. de Vries, S., van Spanning, R. J. M., and Steinebach, V. (2000) *J. Mol. Catal. B: Enzym. 8*, 111−120.
57. Laskowski, R. A., Macarthur, M. W., Moss, D. S., and Thornton, J. M. (1993) *J. Appl. Crystallogr. 26*, 283−291.
58. Cai, D., Dove, J., Nakamura, N., Sanders-Loehr, J., and Klinman, J. P. (1997) *Biochemistry 36*, 11472−11478.
59. Schwartz, B., Green, E. L., Sanders-Loehr, J., and Klinman, J. P. (1998) *Biochemistry 37*, 16591−16600.
60. Lindstrom, A., Olsson, B., and Pettersson, G. (1973) *Eur. J. Biochem. 35*, 70−77.
61. Bellelli, A., Morpurgo, L., Mondovi, B., and Agostinelli, E. (2000) *Eur. J. Biochem. 267*, 3264−3269.
62. Mure, M., and Klinman, J. P. (1995) *Methods Enzymol. 258*, 39−52.
63. Hartmann, C., and Klinman, J. P. (1987) *J. Biol. Chem. 262*, 962−965.
64. Mure, M., and Klinman, J. P. (1993) *J. Am. Chem. Soc. 115*, 7117−7127.
65. Plastino, J., Green, E. L., Sanders-Loehr, J., and Klinman, J. P. (1999) *Biochemistry 38*, 8204−8216.
66. Christopher, J. A. (1997) *SPOCK*, Centre for Macromolecular Design, Texas A&M University, College Station, TX.

BI011187P